JOURNAL OF OPTOELECTRONICS AND ADVANCED MATERIALS Vol. 9, No. 8, August 2007, p. 2430 - 2436

Application of support vector machine for trace gas detection by using temperature-tuning optical parametric oscillator

N. NI[a*], C.C. CHAN[a], J. KONG[a], D.Y. TANG[b]
Network Technology Research Centre, Nanyang Technological University, Research TechnoPlaza, #04-12, XFrontiers Block, 50 Nanyang Drive, Singapore 637553
[a]School of Chemical and Biomedical Engineering, [b]School of Electrical and Electronic Engineering, Nanyang Technological University, Singapore 639798

Support vector machine (SVM), is proposed to enhance the measurement accuracy of a temperature-tuning optical parametric oscillator (OPO) gas sensing system. The experimental results demonstrate that the minimum detecting concentration after the use of SVM decreases by more than 8 times.

(Received May 7, 2007; accepted June 27, 2007)

Keywords: Optical parametric oscillator, Trace gas detection, Support vector machine

1. Introduction

Trace gas detection has attracted highly attention for the application in the fields of environmental monitoring, safety, chemical and biomedical sectors. Laser spectroscopy, based on detecting the unique absorption spectrum as known as "fingerprint" of each species of gas, is a highly sensitive and selective gas sensing technique to identify and quantify particular trace gas. The fingerprint spectra of most organic gases, such as methane, ethane, etc., typically possess the strongest absorption in the mid-infrared wavelength range of 2-5μm, which is, however, not readily accessible with conventional laser sources. Therefore, special mid-infrared laser sources need to be developed to provide coherent radiation with the required features of wide and smooth wavelength coverage, narrow bandwidth and high average power for the laser spectroscopy purpose.

Optical parametric oscillator (OPO) working in the near and mid-infrared wavelength range is a type of promising laser source for the detection of trace gases. Especially, the OPO system based on quasi-phase-matched materials has been well investigated because it can generate near and mid-infrared radiation with wide wavelength tunability and narrow line-width [2-4]. In particular, the periodically poled lithium niobate (PPLN) has attracted much attention because of its large nonlinear optical coefficient [5]. Highly efficient continuous-wave PPLN optical parametric oscillators have been demonstrated and multi-watt output power was obtained [6-8]. Because of the high parametric gain of the OPO, pulsed OPO has also been used to realize high efficient output with relative low pump power. Notwithstanding its advantage of large nonlinear optical coefficient, $LiNbO_3$ is a type of photorefractive material and therefore the PPLN-based OPO has to be operated at elevated temperatures to prevent photorefractive damage. Compared with the conventional $LiNbO_3$, MgO-doped $LiNbO_3$ is more promising to be used in the OPO systems because of the greatly improved resistance to the photorefractive damage [9-10].

Although of those highlights, OPO still has some limitations on the commercial application of trace gas detection. Due to instability of the OPO intensity and non-neglected linewidth compared with that of the gas absorption lines [11], the measurement errors will be induced and thus the sensitivity of the OPO sensing system will be decreased.

To remove those interior measurement errors brought by the gas sensing setup, in this paper, a model based on support vector machine is proposed to process the measurement spectra. Support vector machine, which is a supervised learning method based on the staticstical learning tehory, is applied broadly in the fields of image analysis, signature authentication, text retrieval and face and speech recognition [12]. The principles are described in Section 2, followed by the experimental setup and results which are given in Section 3. Finally, the conclusion is presented in the Section 4.

2. Principles

Optical parametric oscillator (OPO), is proposed to be functioned as a laser source used in trace gas detection in this paper. It is a device that converts a pump wave at frequency ω_p into two lower frequencies of signal and idler waves ω_s and ω_i generated by the driven second order polarization of the nonlinear optical material. Frequencies of the generated waves are determined by energy conservation:

$$\omega_s + \omega_i = \omega_p \tag{1}$$

Since the pump wave can be split into any combination of lower energy signal and idler waves within the constraint of energy conservation, the pump radiation can be shifted to longer wavelengths with wide tunability.

Wavelength or frequency tuning is able to be achieved through the change of temperature. This is because the refractive index of a material is a function of temperature. Indices of some birefringent crystals, e.g., $LiNbO_3$ and LiB_3O_5, are very sensitive to the change of the ambient temperature. The change in temperature will alter the index sphere of ordinary waves and the index ellipsoid of extraordinary waves, then the output will be tuned by varying the crystal temperature. Temperature tuning can be used as a main tuning method for OPOs based on such crystals. The technique has an advantage of not requiring realignment of the cavity since no mechanical change is involved in the process.

When the continuous wave (CW) light from a temperature tuning OPO with initial intensity I_0 passes through a gas sample, the gas molecules absorb photons at specific wavelength and transit from lower to higher vibrational–rotational levels. Thus, the output light intensity denoted as I_t decays at corresponding wavenumber and the molecular absorption spectrum could be detected, followed with Beer's law,

$$I_t = I_0 \exp(-\alpha l C) \tag{2}$$

where l is the effective path-length (cm) of the gas cell, C is the gas concentration (atm^{-1}) and α is the molar absorption coefficient ($atm^{-1}cm^{-1}$). By measuring the molecular absorption spectrum, the concentration of the gas sample could be measured. The measurement error in terms of minimum detection concentration could be estimated by

$$\Delta C_{\min} = C \cdot \frac{\Delta I_A}{I_A} \tag{3}$$

where I_A is the absorption, defined as $I_A=I_0-I_t$. [13]

From Eq. (3), the minimum detection concentration is linear dependent on the change of the absorption, which is influenced by the laser excitation contribution, the noise in the experimental setup, and etc. So, the measurement error will be induced and the measurement accuracy will be also limited.

Support vector machine (SVM), which is based on the strict mathematical theory, is proposed to enhance the measurement accuracy of the aforementioned OPO gas system. SVM is outstanding for solving the linear or nonlinear problem, even reliable at underfitting, overfitting or high noise conditions. The support vector regression (SVR) algorithm is described as below.

A training data set $\{[x(i),y(i)]\in\Re\times\Re, i=1,2,k\}$ consists of k pairs of (x_1,y_1), (x_2,y_2),…, (x_k,y_k), with $x_i\in x\subseteq\Re$, $y_i\in y\subseteq\Re$. In this specific spectral problem, $x(i)$ represents the absorption wavelength at i-th point, $y(i)$ is the corresponding output of transmission defined as the ratio of the output intensity I_t and input intensity I_0. Generally speaking, $y(i)$ should be a nonlinear function of $x(i)$. The objective is to predict the nonlinear function

$$f(x) = \sum_{i=1}^{k} w_i \phi_i(x) + b \tag{4}$$

with the help of an ε–insensitive loss function $L_\varepsilon(x,y,f)$

$$L_\varepsilon(x,y,f) = |y - f(x)|_\varepsilon = \begin{cases} 0 & \text{if } |y-f(x)| \le \varepsilon \\ |y-f(x)| - \varepsilon & \text{otherwise} \end{cases} \tag{5}$$

where w_i and b are the weight and bias coefficients to be solved respectively. As shown in Fig. 1, by using this method, function $f(x)$ has the least deviation larger than ε from the actually obtained target y for all the training data. In other words, the errors as long as less than ε are not considered, but any deviation larger than that will not be acceptable.

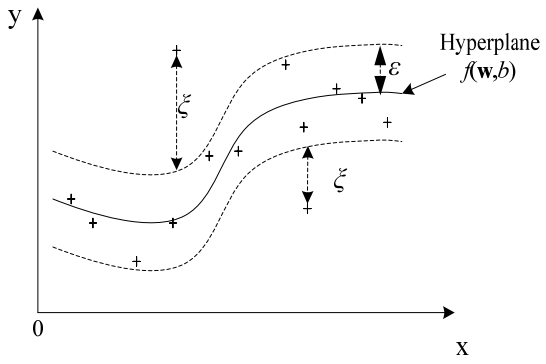

Fig. 1. Nonlinear support vector regression function.

The problem changes to seek the optimal regression function by the minimization of the functional,

$$\Phi(w,\xi,\xi^*) = \frac{1}{2}\|w\|^2 + h\sum_{i=1}^{k}(\xi_i + \xi_i^*) \tag{6}$$

subject to

$$\langle w_i \cdot \phi(x_i)\rangle + b - y_i \le \varepsilon + \xi_i$$
$$y_i - \langle w_i \cdot \phi(x_i)\rangle - b \le \varepsilon + \xi_i^*$$

and

$$\xi_i, \xi_i^* \ge 0, h > 0$$

where $\|w\|^2=\langle w\cdot w\rangle$. The constant h determines the trade-off between the flatness of f and the amount up to which deviation larger than ε are tolerated.

Eq. (6) could be solved by Lagrangian optimization algorithm:
maximize

$$W(\alpha) = -\frac{1}{2}\sum_{i,j=1}^{k}(\alpha_i - \alpha_i^*)(\alpha_i - \alpha_i^*)K(x_i,x_j) - \varepsilon\sum_{i=1}^{k}(\alpha_i + \alpha_i^*) + \sum_{i=1}^{k} y_i(\alpha_i - \alpha_i^*) \tag{7}$$

Subject to

$$\sum_{i=1}^{k}\left(\alpha_i - \alpha_i^*\right) = 0 \text{ and } 0 < \alpha_i^{(*)} \le h$$

and

$$w = \sum_{i=1}^{k}\left(\alpha_i - \alpha_i^*\right)\phi\left(x_i\right) \text{ and } f\left(x\right) = \sum_{i=1}^{k}\left(\alpha_i - \alpha_i^*\right)K\left(x, x_i\right) + b$$

where $\alpha_i^{(*)}$ are Lagrange multipliers and

$$K\left(x, x_i\right) = \left\langle \phi\left(x\right) \cdot \phi\left(x_i\right) \right\rangle$$

is called Kernel function, which controls nonlinear ability of predicted model. Commonly used Kernel function includes linear Kernel, Gaussian Kernel, polynomial Kernel and Sigmoide Kernel. For nonlinear data sets, the Gaussial Kernel and polymomial Kernel are always priority tried in the computation [14].

3. Experimental setup and results

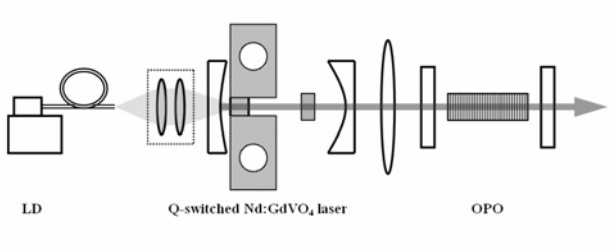

Fig. 2. Schematic of the OPO experimental setup.

The OPO system used in the experiment is schematically shown in Fig. 2. The pump source was a home-made passively Q-switched Nd:$GdVO_4$ laser with a Cr^{4+}:YAG saturable absorber. A commercial laser-diode-bar was used to pump the Nd: $GdVO_4$ laser. The laser diode (LD) pumping light was coupled to a multimode fiber with 600-micron-diameter core and focused into the Nd:$GdVO_4$ sample by two coupling lenses of 1.7cm focal length. The focused pump beam in the laser medium had an average diameter of about 400 μm. The Nd:$GdVO_4$ crystal has a Nd^{3+} doping concentration of 0.5%. It had a dimension of 3×3 mm in cross-section and 4mm in length. An anti-reflection coated Cr^{4+}:YAG crystal with a thickness of 5 mm was applied as saturable absorber. To keep the system thermally stable and prevent possible thermal fracture, both the Nd:GdVO4 crystal and the Cr^{+}:YAG crystal were wrapped with indium foil and mounted in a water-cooled copper crystal holder whose temperature was controlled at about 14 ºC. In order to achieve high conversion efficiency between the pump laser light and the signal wave, high peak power of the pump light was preferred. Several steps were taken to shorten the Q-switching pulse width and increase the peak power. Firstly, the saturable absorber with high initial transmission was used to increase the modulation depth. In the experiments, the initial transmission of the Cr^{4+}:YAG was up to 60%. Secondly, the output coupling was increased as high as 60% and shortened the cavity length to 30 mm to reduce the cavity lifetime of the photons. With these laser parameters, the Q-switched laser can produce pulses as short as 3ns and a repetition rate of 5 kHz at the wavelength of 1063 nm. The characteristics of the Q-switched laser output were monitored and analyzed by a digital oscilloscope (Tektronix TDS 360) with a high speed InGaAs photon detector. Fig. 3 shows a typical Q-switched pulse profile obtained in the build-up laser.

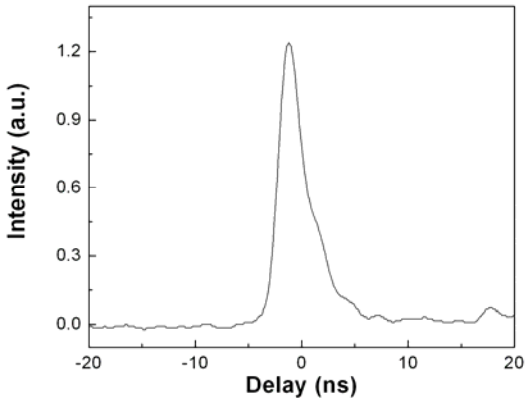

Fig. 3. Oscilloscope trace of the Q-switched pump laser pulse.

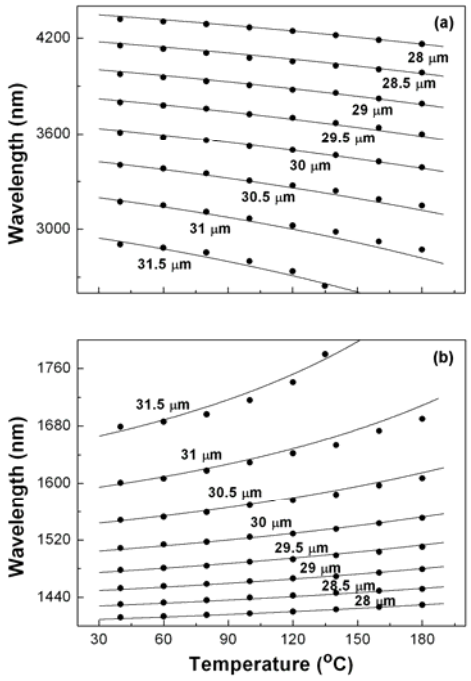

Fig. 4. Temperature tuning curves for 1.064-μm-pumped OPO in PPMgLN with different grating periods: (a) idler wavelength; (b) signal wavelength. Filled circles: experimental data; solid curves: theoretical fitting curves.

The OPO was a single resonant at the signal wave and consisted of two flat mirrors, M_1 and M_2, which were separated by about 50 mm. The input mirror M_1 was a optically coated CaF_2 flat with high reflectivity for the signal wave (R > 98% at 1.5–1.7μm) and idler wave (R>95% at 2.9–3.5 μm) and high transmission (T=90%) at the pump wavelength; the output mirror was a coated CaF_2 flat with high reflectivity for the signal wave (R>95% at 1.5-1.7 μm) and idler wave (R>90% at 2.9-3.5 μm) and transmission (T=30%) at the pump wavelength. A single lens with focal length of 150mm was used to focus the pump beam into the PPMgLN crystal, producing a waist radius of 200μm at the center of the crystal. The multi-grating MgO-doped PPLN crystal (5 mol%) was used as nonlinear medium for the OPO. Two end faces of the crystal were antireflection coated in 1.5-1.7μm for the signal band and 1.064μm for the pump wavelength. The crystal was placed inside an oven with temperature stability of 0.1 ºC. In the experiment, the OPO can be realized with 8 grating periods from 31.5 to 28 μm because of the greatly enhanced peak power of the pump light. The signal wavelength was measured by using an optical spectrum analyzer (OSA, Ando 6317) with a resolution of 0.05nm. With different grating periods and operation temperature, the signal and idler output can be tuned in the range of 1.41-1.78 μm and 2.7-4.3 μm respectively. Fig. 4 shows the temperature-tuning curves of the OPO. The relation between the average signal output power and absorbed pump power was also measured and shown in Fig. 5 and 6. Fig. 6 shows the signal output power versus the absorbed pump power with a 30.5μm grating period at 120 °C crystal temperature which corresponded to the signal wavelength of 1546 nm. The average signal output power was measured to be 35.4 mW at the full pump power of 120 mW. The slope efficiency was calculated to be 30%. It was also found that the signal output power did not change much with different gratings in the range of 1.5-1.7 μm and quickly dropped when the wavelength was below 1.5 μm as shown in Fig. 6. The decreased signal output power was caused by the limitation of the crystal coating.

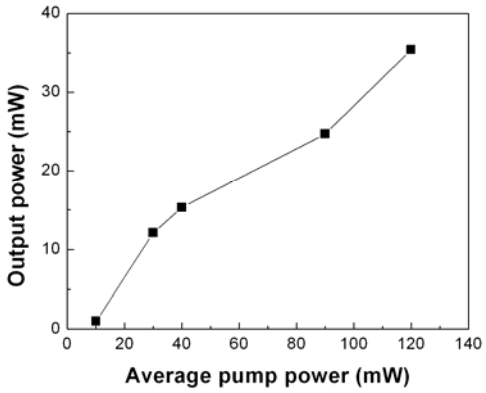

Fig. 5. Signal output power versus input pump power of the OPO with a 30.5μm grating period at 120°C crystal temperature.

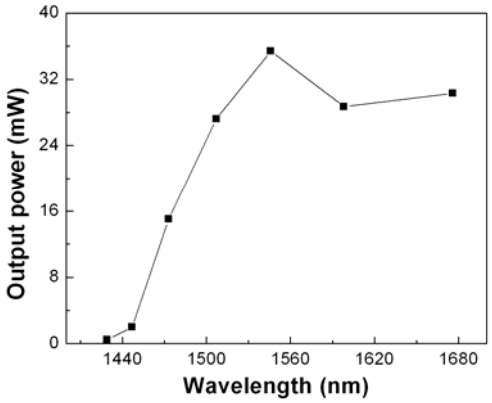

Fig. 6. Signal output power versus input pump power of the OPO with 120 °C crystal temperature and different grating periods at full pump power.

Although the OPO can be tuned from 1.4 μm to 1.76 μm in the signal wavelength and 2.7-4.3 μm in the idler wavelength, it is far from practical application for spectroscopy. Two problems need to be solved before its further application. Due to the intrinsic instability of the passively Q-switched laser, the pump power was not stable with the time. Correspondingly the OPO output power slightly changed from time to time. In addition, neither the pump laser cavity nor the OPO cavity contained any etalons to control the wavelength performance. Thus, the line-width of the signal wavelength was up to 0.5nm and mode-hoping always occurred in the system. To conquer the former problem, a synchronization measuring system was designed and shown in Fig. 7, in which the signal wavelength, reference power and absorbed signal output power could be measured at the same moment.

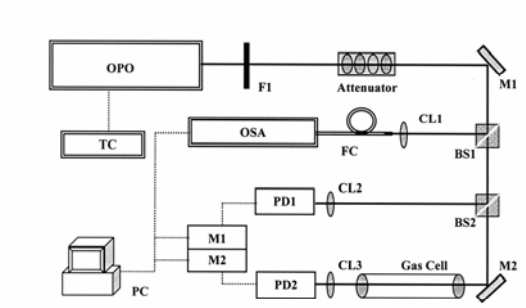

Fig. 7. Schematic of the gas measurement system: F: filter, M: high reflection mirror, BS: beam splitter, CL: coupling lens, FC: fiber coupler, PD: photo detector, M: multimeter, TC: temperature controller, PC: personal computer.

As shown in Fig. 7, a filter was used to block the pump light and idler wave and pass the signal wave. The signal wave was sampled in a beam splitter (BS1) to the OSA. Another beam splitter (BS2) separated the signal wave into two parts. Part 1 was detected by photo detector

1 (PD1) directly which served as the reference light. PD2 detected the absorbed signal light after passing through a gas cell. The signal and reference light were collected respectively by two focal lenses (CL1 and CL2) and coupled to the photo detectors. The incident signal and reference light power were measured with two digital multimeters respectively. A computer was used to control the digital multimeters and the OSA. By changing the crystal temperature through the temperature controller, the OPO could produce tunable signal output. At the same time, the PC controlled the digital multimeters and the OSA to read the data at the same time point with a certain time interval. Since the reflectivity of BS2 had been accurately measured, the signal power of Part 2 before passing the gas cell could be calculated according to the measured reference light power. By using this type of configuration, the effect caused by the fluctuation of the signal output power was fully eliminated. Similarly, since the signal wavelength was measured at the same time with the absorbed signal power, the effect caused by the mode hoping of the OPO had been greatly reduced.

The use of the OPO system for spectroscopy was demonstrated by directly measuring the photon absorption spectrum of the methane (CH_4) molecules. Fig. 8(a) shows background spectrum from the reference path 1 and raw absorption data from path 2. Due to existence of the background light, the backline of raw spectrum was nonlinear. After subtracting the background signal, the processed absorption spectrum of CH_4 was much flatter as shown in the Fig. 8(b). The OPO yielded light from 1640 nm to 1680 nm. It shows that CH_4 has several large absorption peaks which are located at 1648.5 nm, 1666.5 and 1674.5 nm respectively.

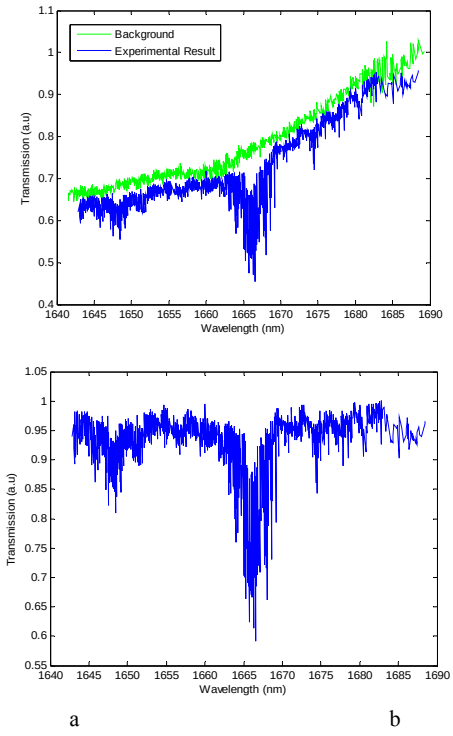

a b

Fig. 8. Measured absorption spectrum of methane.

Although by the synchronization measuring system, the amplitude fluctuation of the OPO brought by the unstability of the pump laser was greatly depressed, the influence of the linewidth of the OPO was still unable to be reduced. Due to the relatively broader linewidth of the OPO compared to that of the gas spectrum, the signal wavelength of some data would be misread. Those misread data would decrease the measurement accuracy of the gas absorption spectra. Furthermore, the OPO gas sensing system and thus the corresponding accuracy of the gas absorption spectra based on this gas sensing system were also limited by the resolution of the OSA. To further improve the measurement accuracy of the gas spectrum, some signal processing techniques should be employed.

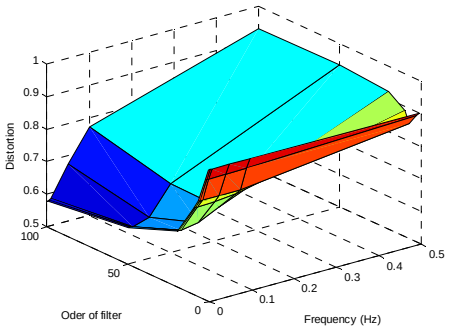

Fig. 9(a): Relationship of distortion after filtering, order of the filter and the cutoff requency.

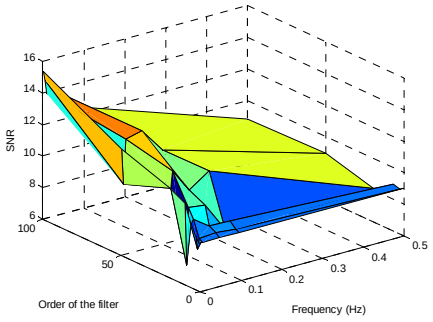

Fig. 9(b): Relationship of SNR after filtering, order of the filter and the cutoff frequency

Finite impulse response (FIR) filter is usually used to remove the noise in sensing system, because of its simple implementation and a linear response [13, 15]. FIR filter operates based on the frequency spectrum of the signal. A discrete Fourier transform (DFT) spectral analysis was employed to the raw spectral data in Fig. 8(b). It was found that most energy of the DFT spectrum of the experimental signal focuses in the low frequency band. A low-pass FIR filter was applied to filter the contaminated signal. The distortion after the filter (the compression of the amplitude of the spectral curve after filtering compared with that before the filter) and the signal to noise ratio

(SNR) defined as $I_A/\Delta I_A$ with the change of the order and cutoff frequency of the filter were investigated respectively. Fig. 9 demonstrated the filtered signal became smoother with the price of amplitude distortion. With an acceptable distortion and a relative high SNR, the length and cut-off frequency of the filter were selected as 7 and 0.001Hz respectively. The result after that designed filter is shown in Fig. 10. The SNR was increased from 4 to 10, only about 3 times enhanced than that before filtering, while the distortion ratio achieved to be 0.81.

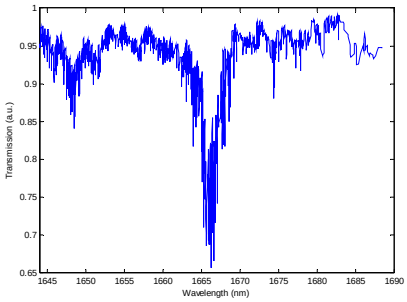

Fig. 10. CH_4 absorption spectrum after the FIR filter with order of 7 and cutoff frequency of 0.001Hz.

The unsatisfactory filtered result is due to this sort of filter which is based on the spectral properties of the signal and noise. However, the contaminated signals own the similar spectral property to the ideal signals. In this case, FIR filter is not quite suitable in the use of the OPO gas sensing system.

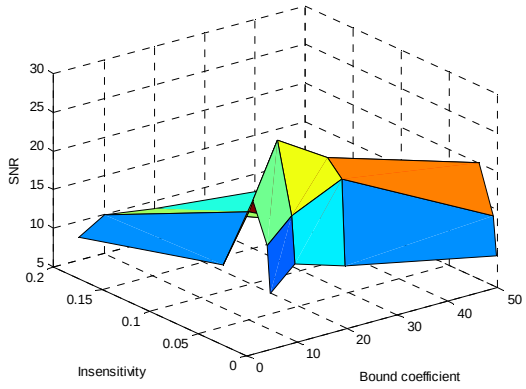

Fig. 11. Relationship of the SNR after SVM, trade-off coefficient and the insensitivity.

Alternatively, SVM was employed to enhance the measurement accuracy of the sensing system. Kernel function was selected to be Gaussian with standard deviation 0.001 due to the property of the gas spectrum. The relationship of the other SVM parameters (such as the bound coefficient h and insensitivity ε) and the corresponding SNR was discussed as in Fig. 11. It was found that when the insensitivity was set to be 0.02, and bound coefficient was equal to 10, the SNR was achieved maximum, equal to 30, thus the corresponding minimum detecting concentration was decreased 8 times than that before the processing. The gas spectrum result after processing is illustrated as Fig. 12. The curve after process was more smooth and reasonable compared with the spectrum from the supplier. The smooth curve after the processing also proved the effectivity of the SVM in the OPO sensing problem compared with FIR algorithm.

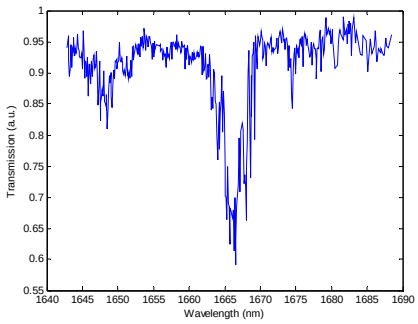

Fig. 12. Processed spectral result after using support vector regression.

4. Conclusions

The possibility of using an efficient compact singly resonant optical parametric oscillator (OPO) for trace gas detection is presented by measuring the absorption spectra of CH_4. Support vector machine is used to reduce the influence brought by the confinement of the light source and the noises in this sensing system. After the use of SVM, the SNR is enhanced 8 times than that before processing, although the improvement is limited due to the high contamination of the raw signal and thus the SVM algorithm could not distinguish and erase all the misread data. The enhancement the measurement accuracy demonstrates that, SVM is a compatible and promising technique used in the OPO gas sensing system.

References

[1] R. F. Curl, F. K. Tittel, Annu. Rep. Prog. Chem. Sect C **98**, 219 (2002).
[2] K. A. Tillman, R. R. J. Maier, D. T. Reid, E.D. Mcnaghten. J. Opt. A: Pure Appl. Opt. **7**, S408 (2005).
[3] A. Popp, F. Müller, F. Kühnemann, S. Schiller, G. Basum, H. Dahnke, P. Hering, M. Mürtz, Appl. Phys. B, **75**, 751 (2002).
[4] K. W. Anioleka, P. E. Powersb, T. J. Kulp, B.A. Richmana, S.E. Bissona, Chem. Phys. Lett., **302**, 555 (1999).
[5] L. E. Myers, R. C. Eckardt, M. M. Fejer, R. L. Byer, W.R. Bosenberg, J.W. Pierce, J. Opt. Soc. Am. B, **12**, 2102 (1995).
[6] Van Herpen, Te Lintel Hekkert, S.E. Bisson, F. Harren, Opt. Lett., **27**, 640 (2002).

[7] Van Herpen, S. Li, S.E. Bisson, Te Lintel Hekkert, F. Harren, Appl. Phys. B, **75**, 329 (2002).
[8] Van Herpen, S.E. Bisson, A. Ngai1, F. Harren, Appl. Phys. B, **78**, 281 (2004).
[9] D. Y. Shen, S. C. Tam, Y. L. Lam, T. Kobayashi, Electron. Lett., **36**, 1488 (2000).
[10] H. P. Li, D. Y. Tang, S. P. Ng, J. Kong, Opt. Laser. Technology, **38**, 192 (2006).
[11] L. S. Rothman, D. Jacquemart, A. Barbe etc., J. of Quantitative spectroscopy & Radiative Transfer, **96**, 139 (2005).
[12] S. Theodoridis, K. Koutroumbas, Pattern recognition, 2003 Elsevier Science USA, pp. 1-8.
[13] N. Ni, C. C. Chan, J. Optoelectron. Adv. Mater. **8**(4), 1613 (2006).
[14] N. Chen, W. Lu, J. Yang, C. Li, Support vector machine in Chemistry. World Scientific 2004, pp.24-58.
[15] C. C. Chan, W. Jin, M. S. Demokan, Optics&Laser Technology, **31**, 299 (1999).

*Corresponding author: nina@pmail.ntu.edu.sg